Patch-Based Image Deblocking Using Geodesic Distance Weighted Low-Rank Approximation

Mading Li, Jiaying Liu*, Jie Ren and Zongming Guo

Institute of Computer Science and Technology, Peking University, Beijing, P. R. China, 100871

*liujiaying@pku.edu.cn

Abstract—Transform coding based on the discrete cosine transform (DCT) has been widely used in image coding standards. However, the coded images often suffer from severe visual distortions such as blocking artifacts. In this paper, we propose a novel image deblocking method to address the blocking artifacts reduction problem in a patch-based scheme. Image patches are clustered and reconstructed by the low-rank approximation, which is weighted by the geodesic distance. Experimental results show that the proposed method achieves higher PSNR than the state-of-the-art deblocking and denoising methods and the processed images present good visual quality.

Index Terms—Image deblocking, patch-based, low-rank approximation, geodesic distance, reconstruction

I. INTRODUCTION

With the rapid development of the multimedia technology, tons of image and video resources are being spread through all kinds of means on the Internet everyday. To make the full use of the limited bandwidth, transform coding, *e.g.* the block-based discrete cosine transform (BDCT) has been widely used to compress images and videos. However, due to the fact that each block of the image is transformed and quantized independently in BDCT, the compressed image often suffers from severe degradation especially around block boundaries. Such degradation is known as the blocking artifacts, which becomes more serious when the bit rate is low.

In order to alleviate the blocking artifacts, many revealing studies and researches have been performed in recent decades. One of the most intuitive ways is to smooth the block boundaries directly by a deblocking filter. This kind of methods required minimum computational cost and could be implemented easily. However, these methods were limited to block boundaries and ignored the prior knowledge of natural images. The other kind of methods tended to restore the image and considered the deblocking process as an inverse problem of the initial BDCT operation. Therefore, the prior knowledge of the image could be well utilized in the restoration procedure. The projection onto convex sets (POCS) based methods are the representative research of this kind of

methods for deblocking. Foi *et al.* [1] proposed an image restoration filtering algorithm based on the shape-adaptive DCT (SA-DCT). In this method, the adaptive support for the transform produced clean reconstructed edges while reducing the unpleasant ringing and blocking artifacts.

Although these methods can achieve good deblocking performances, the correlations between similar patches are neglected. It is well known that there exists redundant information in natural images. In recent years, the self-similarity property in natural image and video signals has been widely explored, especially in the image restoration field. Ji *et al.* [2] proposed a video denoising method using the self-similarity. By clustering similar patches and solving a low-rank matrix completion problem, their method presented good performance dealing with mixed noise.

In this respect, blocking artifacts can be regarded as a specific noise and be solved by the denoising method since decoded images still have redundant information. Nevertheless, blocking artifacts are different from general noises after all. Blocking artifacts appear mostly on the boundaries of the image blocks and the intensity distortion is less than general noises. In addition, blocking artifacts somehow blur the image blocks and degrade the performance of the patch clustering. In this paper, we propose a novel image deblocking method. Since the redundant information in decoded images has rarely been utilized in deblocking methods, we present the proposed method in the following steps. By clustering similar patches, we can obtain a matrix that should be low-rank. Then we use the singular value thresholding (SVT) algorithm [3] to solve the low-rank approximation problem. After that, to compensate for the mismatch of the clustering procedure caused by blocking artifacts, geodesic distance is utilized to weight different patches in the matrix. At last, we relocate the updated patches back to the image.

The rest of the paper is organized as follows: Section I introduces the deblocking problem and gives a brief overview of the proposed method. The details of the method, including patch clustering procedure, low-rank approximation algorithm and geodesic distance weighting method are presented in the following subsections. Experimental results are demonstrated in Section III, which show the state-of-the-art quality of the final deblocking results of the proposed method, both in terms of objective criteria and visual quality. Finally, Section IV concludes the paper.
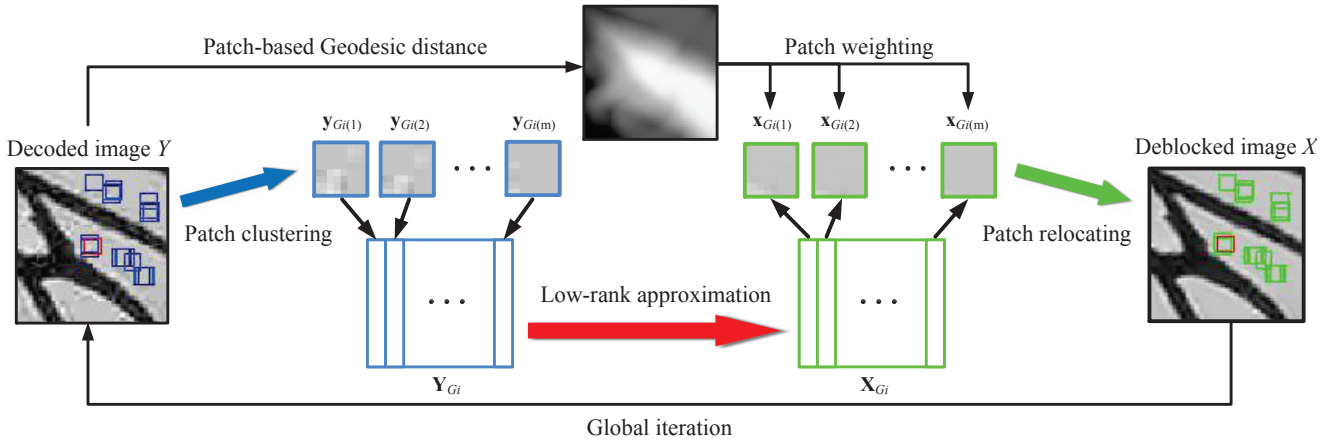
Fig. 1.   The flowchart of the proposed patch-based image deblocking method.

II. PATCH-BASED IMAGE DEBLOCKING METHOD

A. Problem Formulation

The BDCT compressed image can be modeled as corrupted one with the quantization noise as follows

$$Y = X + E, \tag{1}$$

where X is the original image, Y is the compressed blocky image and E is the quantization noise. In this paper, we adopt a patch-based scheme to reconstruct X from Y by reducing E. Let y_i denote a small image patch of size $\sqrt{n} \times \sqrt{n}$, located in position i in image Y. The corresponding clean image patch is denoted by x_i. Then we have the following equation:

$$y_i = x_i + e_i, \tag{2}$$

where e_i is the quantization noise for the image patch x_i. For each patch y_i in the input decoded image Y, a group of similar patches is collected. The whole group is formed into a data matrix. According to the self-similarity property of natural images, all the non-local similar patches have similar underlying image structures. Therefore, the rank of the data matrix should be low. As shown in Fig.1, our deblocking method applies the low-rank approximation to each data matrix constructed by the local patch clustering. Then the processed data matrix weighted with the geodesic distance is reformed into image patches and relocated to their original positions. Finally, by aggregating the processed patches with overlapped region, an estimation of the original image X is obtained and it can be used as the input for the following iteration.

B. Patch Clustering

For the compressed image Y, we set patch y_i as the reference patch and search for patches that are similar to y_i within a neighborhood of position i, $\Omega(i)$. The indices of these similar patches are grouped into G_i, which is

$$G_i = \{j \mid T \geq \|y_i - y_j\|_2, j \in \Omega(i)\}, \tag{3}$$

where the parameter T controls the minimum degree of the similarity among patches. Assuming that m similar patches have been found, we can define an $n \times m$ data matrix $\mathbf{Y}_{G_i}$ as follows,

$$\mathbf{Y}_{G_i} = (\mathbf{y}_{G_i(1)}, \mathbf{y}_{G_i(2)}, \ldots, \mathbf{y}_{G_i(m)}), \tag{4}$$

where $\mathbf{y}_{G_i(k)}$ is an $n \times 1$ vector containing all columns of the k_{th} similar patch. Then we can rewrite Eqn.(2) as:

$$\mathbf{Y}_{G_i} = \mathbf{X}_{G_i} + \mathbf{E}_{G_i}, \tag{5}$$

where $\mathbf{X}_{G_i}$ represents the data matrix consisting of the original image patches and $\mathbf{E}_{G_i}$ represents the quantization noise.

C. Low-Rank Approximation

As described above, the data matrix $\mathbf{X}_{G_i}$ should have low-rank structure. Given the corrupted data matrix $\mathbf{Y}_{G_i}$, $\mathbf{X}_{G_i}$ can be restored by solving the standard low-rank minimization problem:

$$\begin{aligned} &\min rank(\mathbf{X}_{G_i}), \\ &\text{s.t. } \|\mathbf{X}_{G_i} - \mathbf{Y}_{G_i}\|_F^2 < c \cdot \sigma_E, \end{aligned} \tag{6}$$

where σ_E is the variance of the quantization noise, $\|\cdot\|_F$ denotes the Frobenius norm and c is a scaling factor for the error tolerance.

Since the low-rank minimization problem in Eqn.(6) is an NP-hard problem and cannot be solved efficiently, we consider its tightest convex relaxation instead:

$$\begin{aligned} &\min \|\mathbf{X}_{G_i}\|_*, \\ &\text{s.t. } \|\mathbf{X}_{G_i} - \mathbf{Y}_{G_i}\|_F^2 < c \cdot \sigma_E, \end{aligned} \tag{7}$$

where $\|\mathbf{X}_{G_i}\|_*$ represents the nuclear norm of matrix $\mathbf{X}_{G_i}$, which is equal to the sum of the singular values σ_j of matrix $\mathbf{X}_{G_i}$, $\|\mathbf{X}_{G_i}\|_* = \sum_j \sigma_j(\mathbf{X}_{G_i})$. Many numerical low-rank approximation algorithms can be utilized to solve the minimization problem in Eqn.(7). In this paper, we use the Singular Value Thresholding (SVT) algorithm [3] for its simplicity and ease of implementation.

The SVT algorithm starts with $\mathbf{X}_{G_i}^0 = \mathbf{Y}_{G_i}$, and iterates between two steps as follows:

$$\begin{cases} \mathbf{Z}^k = D_\tau(\mathbf{X}_{G_i}^{k-1}), \\ \mathbf{X}_{G_i}^k = \mathbf{X}_{G_i}^{k-1} + \delta(\mathbf{Y}_{G_i} - \mathbf{Z}^k), \end{cases} \tag{8}$$

where $D_\tau(\cdot)$ denotes the soft shrinkage operator and δ is an iterative regularization factor controlling the feedback of filtered noise. Let $Q = U\Sigma V^T$ be the SVD for Q, then $D_\tau(Q)$ is defined as:

$$D_\tau(Q) = U\Sigma_\tau V^T, \qquad (9)$$

where $\Sigma_\tau = diag(\max(\sigma(Q) - \tau, 0))$. $\sigma(Q)$ denotes the singular values of matrix Q and τ is the threshold for the soft shrinkage operation.

As demonstrated in [4], under the assumption of Laplacian prior, the thumb rule for choosing the threshold τ in Eqn.(8) is $\tau = 2\sqrt{2} \cdot \sigma_E^2 / \sigma_{\mathbf{X}_{G_i}}$, in which $\sigma_{\mathbf{X}_{G_i}}$ denotes the locally estimated signal variance given as follows:

$$\sigma_{\mathbf{X}_{G_i}} = \sqrt{\max(\sigma^2(\mathbf{X}_{G_i}^0)/m - \sigma_E^2, 0)}, \qquad (10)$$

where $\sigma(\mathbf{X}_{G_i}^0)$ denotes the singular values of $\mathbf{X}_{G_i}^0$. In the iteration procedure of Eqn.(8), the noise variance and signal variance should be updated because the quantization noise has been reduced in each iteration. We use the suggestion in [5] to update the two variances:

$$\sigma_E^{(k)} = \gamma\sqrt{\sigma_E^2 - \|\mathbf{X}_{G_i}^0 - \mathbf{X}_{G_i}^{k-1}\|_2}, \qquad (11)$$

$$\sigma_{\mathbf{X}_{G_i}}^{(k)} = \sqrt{\max(\sigma^2(\mathbf{X}_{G_i}^{k-1})/m - (\sigma_E^{(k)})^2, 0)}, \qquad (12)$$

where γ is a scaling factor controlling the re-estimation of the noise variance and σ_E^2 is the quantization noise variance. The details are presented in Section III-B. Therefore, the thresholds τ can be updated by

$$\tau^{(k)} = 2\sqrt{2}(\sigma_E^{(k)})^2 / \sigma_{\mathbf{X}_{G_i}}^{(k)}. \qquad (13)$$

D. Patch-Based Geodesic Distance Weighting

In some cases, the patch clustering may produce undesirable results. Fig.2(b) (a portion of Lena image) shows an example of undesirable clustering results B_1 and B_2 of the reference patch R. B_1 and R come from the same region (the frame of the mirror in the image) while B_2 is actually a part of Lena's hair. Although the intensities of B_1 and B_2 seem close to R, they have relatively different textures. Blocking artifacts somehow make them look the same. In order to solve this problem, we adopt a weighting method based on the geodesic distance to compensate for the mismatch of the clustering procedure. Patch-based geodesic distance defines a path of approximately constant intensity connecting two patches. If two patches have a low geodesic distance, they basically lie in the same region of the image. Thus, we give patches high weights in the aggregation if they lie in the same region with the reference patch.

The patch-based geodesic distance $d^{pGD}(i,j)$ between the reference patch y_i and patch y_j is defined as a shortest path connecting y_i and y_j in the intensity sense [6]:

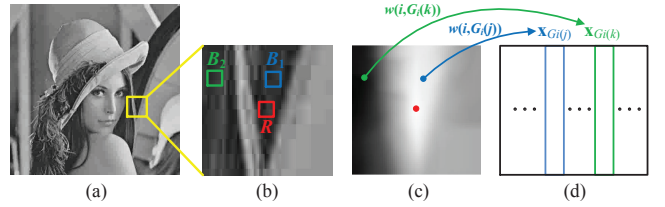$$d^{pGD}(i,j) = \min_{p \in \Gamma_{i,j}} d(p), \qquad (14)$$

Fig. 2. Undesirable clustering results and the geodesic distance weighting. (b) is the enlargement of a local region of the Lena image (a). The red block R represents the reference patch; The blue block B_1 and the green one B_2 represent the j_{th} and the k_{th} similar patch with the reference patch, respectively. (c) is the geodesic distance map of (b), which is used to weight the processed data matrix (d).

where $\Gamma_{i,j}$ denotes the set of all the paths between y_i and y_j. A path p defines a sequence of neighboring positions in 8-connectivity. The cost of p is defined as follows

$$d(p) = \sum_{i=1}^{n_p - 1} \|y_{p_i} - y_{p_{i+1}}\|_2, \qquad (15)$$

where n_p is the number of positions on the path p.

Finally, the weight between patches is given by

$$w(i,j) = e^{-d^{pGD}(i,j)/\varepsilon}, \qquad (16)$$

with ε being a parameter that controls the importance of the geodesic distance weight.

In Eqn.(8), the iterative regularization is performed on each clustered data matrix $\mathbf{Y}_{G_i}$ to restore the clean data matrix $\mathbf{X}_{G_i}$. The whole image can be restored by aggregating all the overlapped patches after each cluster is processed. However, in order to utilize the updated data for the patch clustering and accelerate the convergence of the above iterative procedure, a global iteration is adopted.

First we perform SVT on each $\mathbf{Y}_{G_i}$, $i \in \Psi$, where Ψ contains all the possible positions for reference patches. For each intermediate $\mathbf{X}_{G_i}^k = (\mathbf{x}_{G_i(1)}, \mathbf{x}_{G_i(2)}, \ldots, \mathbf{x}_{G_i(m)})$, we assign geodesic distance weights for it as follows

$$\mathbf{X}_{G_i}^k{}' = (w(i, G_i(1)) \cdot \mathbf{x}_{G_i(1)}, \ldots, w(i, G_i(m)) \cdot \mathbf{x}_{G_i(m)}), \quad (17)$$

and aggregate all the weighted $\mathbf{X}_{G_i}^k{}'$ into a whole image, that is, reform $w(i, G_i(k)) \cdot \mathbf{x}_{G_i(k)}$ to the $\sqrt{n} \times \sqrt{n}$ patch and relocate it back to its position $G_i(k)$ (refer to Fig.1). Then the global iterative regularization on the whole image is applied to produce the input for next iteration. The maximal number of iteration is set to be 10.

III. EXPERIMENTAL RESULTS

A. Experiments Setup

The experiments are implemented on MATLAB platform. Three typical images are used for the tests: Lena, Barbara and House. Three quantization tables, denoted as **Q1**, **Q2** and **Q3** used by [7] have been adopted in order to simulate various types of BDCT compression.

The original test images are coded by the three quantization tables and then reconstructed by the state-of-the-art image deblocking methods (FoE [7], SA-DCT [1]), denoising methods (the classic BM3D [8] and the recent improved version NL-Bayes [9]) and the proposed method.

B. Quantization Noise Variance Estimation

In order to apply the low-rank minimization deblocking algorithm, we need a suitable value for the quantization noise variance σ_E^2. In our experiments, the noise variance σ_E^2 is set as in [1]:

$$\sigma_E^2 = 0.69 \cdot (\tilde{q})^{1.3}, \tilde{q} = 1/9 \sum_{i,j=1}^{3} q_{i,j}, \qquad (18)$$

where the quantization table $Q = [q_{i,j}]_{i,j=1,\dots,8}$ and the mean value $\tilde{q}$ uses only nine of the quantization table entries which correspond to the lowest-frequency DCT harmonics (including the DC-term).

C. Deblocking Results

In Table I, we present results for deblocking from BDCT quantization using the three specific quantization tables **Q1**,**Q2** and **Q3**. We compare the results obtained by the proposed algorithm with the results obtained by the state-of-the-art methods [1], [7], [8], [9]. From Table I we can conclude that the proposed algorithm outperforms most of the methods in terms of Peak Signal-to-Noise Ratio (PSNR). Also, the state-of-the-art denoising methods cannot obtain satisfactory deblocking results since there are significant differences between blocking artifacts and regular noises.

We also compare the visual quality of these four methods in Fig.3. Portions of Lena and Barbara at quantization tables **Q1** and **Q2** are illustrated. The proposed method has the best visual quality against all the other methods, especially along the edge structures. The blocking artifacts are mostly suppressed in the outputs of the proposed method.
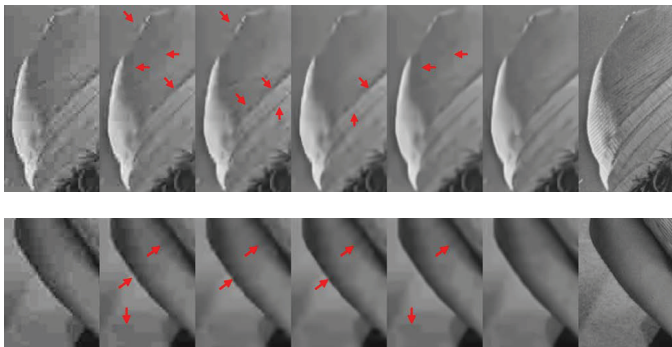

Fig. 3. The portions of deblocking results of Lena and Barbara compressed by quantization tables **Q1** and **Q2**, respectively. From left to right: the decoded image, NL-Bayes, FoE, SA-DCT, BM3D, the proposed method, the clean image. The red arrows point out the unsatisfactory artifacts.

TABLE I
PSNR (DB) RESULTS OF DIFFERENT METHODS FOR QUANTIZATION
TABLES **Q1**,**Q2** AND **Q3**.

Images	Decoded	[7]	[1]	[8]	[9]	Proposed
House	35.13	36.12	36.31	36.36	35.69	**36.44**
	34.53	35.78	35.80	35.81	35.27	**36.03**
	32.78	33.38	33.36	33.38	33.15	**33.54**
Lena	34.97	35.98	35.61	36.01	35.62	**36.09**
	34.40	35.53	35.16	35.45	35.06	**35.58**
	32.94	**34.01**	33.69	33.82	33.59	33.98
Barbara	32.47	33.00	33.14	33.27	32.85	**33.30**
	32.13	32.71	32.81	32.90	32.50	**32.94**
	31.14	31.78	31.85	31.74	31.61	**31.98**
Average	33.39	34.25	34.19	34.30	33.93	**34.43**

IV. CONCLUSION

In this paper, we propose a patch-based image deblocking method using geodesic distance weighted low-rank approximation. By clustering similar patches, a low-rank data matrix can be obtained. The singular value thresholding (SVT) algorithm is applied to solve the low-rank approximation problem. To compensate for the mismatch of the clustering procedure, patch-based geodesic distance is utilized to weight different patches in the data matrix. At last, we relocate the updated patches back to the image. Experimental results show that the proposed method achieves higher PSNR than the state-of-the-art deblocking and denoising methods and the processed images present good visual quality.

REFERENCES

[1] A. Foi, V. Katkovnik, and K. Egiazarian, "Pointwise shape-adaptive DCT for high-quality denoising and deblocking of grayscale and color images," *Image Processing, IEEE Transactions on*, vol. 16, no. 5, pp. 1395–1411, 2007.

[2] H. Ji, C. Liu, Z. Shen, and Y. Xu, "Robust video denoising using low rank matrix completion," in *Computer Vision and Pattern Recognition (CVPR), 2010 IEEE Conference on*. IEEE, 2010, pp. 1791–1798.

[3] J.-F. Cai, E. J. Candès, and Z. Shen, "A singular value thresholding algorithm for matrix completion," *SIAM Journal on Optimization*, vol. 20, no. 4, pp. 1956–1982, 2010.

[4] S. G. Chang, B. Yu, and M. Vetterli, "Adaptive wavelet thresholding for image denoising and compression," *Image Processing, IEEE Transactions on*, vol. 9, no. 9, pp. 1532–1546, 2000.

[5] X. Li, W. Dong, and G. Shi, "Nonlocal image restoration with bilateral variance estimation: a low-rank approach," *Image Processing, IEEE Transactions on*, vol. 22, pp. 700 – 711, 2013.

[6] X. Chen, S. B. Kang, J. Yang, and J. Yu, "Fast patch-based denoising using approximated patch geodesic paths," in *Computer Vision and Pattern Recognition (CVPR), 2013 IEEE Conference on*. IEEE, 2013, pp. 1211–1218.

[7] D. Sun and W.-K. Cham, "Postprocessing of low bit-rate block DCT coded images based on a fields of experts prior," *Image Processing, IEEE Transactions on*, vol. 16, no. 11, pp. 2743–2751, 2007.

[8] K. Dabov, A. Foi, V. Katkovnik, and K. Egiazarian, "Image denoising by sparse 3-D transform-domain collaborative filtering," *Image Processing, IEEE Transactions on*, vol. 16, no. 8, pp. 2080–2095, 2007.

[9] M. Lebrun, A. Buades, and J.-M. Morel, "A nonlocal bayesian image denoising algorithm," *SIAM Journal on Imaging Science*, vol. 6, no. 3, pp. 1665–1688, 2013.